Title

Seismic monitoring of CO2 geosequestration using multi-well 4D DAS VSP: Stage 3 of the CO2CRC Otway project

Authors

Yurikov, Alexey

Tertyshnikov, Konstantin

Yavuz, Sinem

et al.

Publication Date

2022-09-01

DOI

10.1016/j.ijggc.2022.103726

Seismic monitoring of CO_2 geosequestration using multi-well 4D DAS VSP: Stage 3 of the CO2CRC Otway project

Alexey Yurikov[1], Konstantin Tertyshnikov[1], Sinem Yavuz[1], Pavel Shashkin[1], Roman Isaenkov[1], Evgenii Sidenko[1], Stanislav Glubokovskikh[2], Paul Barraclough[3], and Roman Pevzner[1]

[1] Centre for Exploration Geophysics, Curtin University, GPO Box U1987, Perth, WA, 6845, Australia.

[2] Lawrence Berkeley National Laboratory, 1 Cyclotron Road, Berkeley, CA, 94720, USA.

[3] CO2CRC, 11-15 Argyle Place South, Carlton, VIC, 3053, Australia.

Keywords

CCUS; reservoir monitoring; fibre-optics; time-lapse seismic data

Abstract

An important part of any CO_2 geosequestration project is to ensure CO_2 containment and conformance in the subsurface. This is generally done by implementing a comprehensive, risk-based Measurement, Monitoring and Verification plan, a key element of which is active time-lapse seismic monitoring. However, high cost and environmental impact of the standard surface seismic monitoring dictate the need for a cost-effective and environmentally friendly alternative. An opportunity to develop such method emerges with advances in distributed acoustic sensing (DAS) technology, which turns an optical fibre into a seismic sensor with dense spatial sampling. DAS can be permanently deployed in multiple wells across the geosequestration site providing a robust and non-intrusive network of seismic receivers. This approach was developed and tested in the CO2CRC Otway project, where injection of 15 kt of CO_2 at 1.5 km depth was monitored with a 4D vertical seismic profiling (VSP) using five borehole DAS arrays and mobile vibroseis sources. The 4D DAS VSP in each of the five wells provides broadly consistent images of the CO_2 plume with some differences due to different illumination of the target horizon, lateral variation of velocities, and seismic anisotropy. When the newly injected CO_2 reaches a CO_2 plume created as a result of an earlier

injection into the same formation ~600 m updip, 4D DAS VSP shows a change in reflectivity in that area and beyond. This shows a potential of 4D DAS VSP for monitoring gas injection into gas-saturated reservoirs.

Introduction

Carbon capture, utilisation, and storage (CCUS) technology is globally perceived as an important contributor to the reduction of carbon emissions (IEA, 2012, 2021; IPCC, 2021; Pacala and Socolow, 2004; Schrag, 2007). As CCUS involves injecting CO_2 into the subsurface rock formations, an important part of such projects is monitoring and verification (M&V) of CO_2 containment and conformance (Jenkins et al., 2015; Oldenburg, 2018). Several projects have demonstrated that M&V can be fulfilled by means of 4D seismic monitoring (e.g., Bauer et al., 2019; Bourne at al., 2014; Chadwick et al., 2010; Dean and Tucker, 2017; Lüth et al., 2017; Pevzner et al., 2017; Roach and White, 2018) by detecting changes in elastic properties of subsurface layers that are caused by changes in fluid saturation or pressure (Landrø et al., 2003; Lumley, 2001). However, application of the standard 4D surface seismic monitoring has several challenges. First, it requires frequent snapshots of the subsurface, which may be prohibitively expensive (Mathieson et al., 2011). Second, it has large surface footprint and thus can disrupt activities of other users of land or marine resources. Consequently, 4D seismic vintages are acquired several years apart from each other and require significant time for processing, which may be inadequate for M&V purposes.

The demand for cost-effective and less disruptive seismic monitoring methods may be satisfied by using permanently installed seismic receivers. Burying receivers in shallow subsurface not only reduces the footprint of acquisition and mobilisation time, but also improves data repeatability and signal-to-noise (S/N) ratio (Jervis et al., 2018; Pevzner et al., 2017). The invasiveness of seismic acquisition and noise levels can be further reduced if seismic receivers are permanently deployed in boreholes. Application of vertical seismic profiling (VSP) for CO_2 injection monitoring in the Illinois

Basin–Decatur Project (Bauer et al., 2019; Couëslan et al., 2013), Weyburn Field (Majer et al., 2006) , and Otway Project (Correa et al., 2019, 2017; Tertyshnikov et al., 2018) has shown promising results.

Borehole seismic monitoring becomes even more attractive with development of fibre-optic DAS (Hartog, 2017; Parker et al., 2014). This is a relatively new technology that turns an optical fibre into a seismic sensor, which can be deployed along the full extent of a well providing dense spatial sampling. Because fibre-optic DAS can cover the entire well at once, the rig time required for DAS VSP operations is minimal, and hence the cost of the monitoring is significantly lower than when borehole geophones are used. Additionally, fibre optics are more robust than geophones and avoid risks associated with the deployment of mechanical and electrical components into a well. However, DAS has limitations: it captures only a single component of the wavefield (strain along the fibre), and its amplitude response has a $\cos^2$ dependence on an angle of incidence rather than cos for geophones (Li et al., 2015).

In recent years, fibre-optic DAS technology has been tested in several projects, which demonstrated the high potential of DAS VSP for reservoir monitoring (Bacci et al., 2017; Correa et al., 2019, 2017; Daley et al., 2016, 2013; Hopkins et al., 2021; Mateeva et al., 2017; Michael et al., 2020; White et al., 2019; Zwartjes et al., 2018). It has been shown that quality of 3D DAS VSP seismic images can be comparable or sometimes superior to the quality of images obtained using borehole geophone data (Correa et al., 2017). In comparison with surface seismic monitoring, 4D DAS VSP data can be of somewhat lower quality and limited extent (Correa et al., 2019; Mateeva et al., 2017; White et al., 2019). To increase illumination of the subsurface, Mateeva et al. (2017) suggested combining images from several wells and using multiples for imaging. Yurikov et al. (2021) showed that combining images obtained from data recorded in several wells may be challenging because of amplitude artefacts due to uneven fold in a VSP geometry and mis-ties due to inaccuracy of the velocity model used for imaging.

Further development and testing of DAS as a tool for reservoir monitoring is being undertaken within the scope of the CO2CRC Otway project. The project employs multi-well 4D DAS VSP for monitoring of 15 kt of CO_2 injected at the depth of 1.5 km. Here we describe details of acquisition and processing of the multi-well 4D VSP data. Then, we present the analysis of the time-lapse images of the CO_2 plume, cross-validate them with other seismic monitoring methods used in the Otway project and discuss challenges and limitations of 4D DAS VSP as an onshore monitoring tool.

CO2CRC Otway project

The CO2CRC Otway project is the first Australian demonstration of CCUS as a means for carbon emission reduction. The Otway International Test Centre (OITC), the project site, is located in the Australian state of Victoria about 240 km south-west of the city of Melbourne. OITC started its operation in 2003 and now it has seven purpose-drilled wells (>1.5 km deep), within a ~1 km^2 area, for CO_2 injection and monitoring activities.

The Otway Stage 2C Project focused on understanding the effectiveness of various seismic techniques for monitoring CO_2 and demonstrating migration and stabilisation of the CO_2 plume in the subsurface (Cook, 2014). For this purpose, 15 kt of CO_2 were injected into a saline aquifer at a depth of 1.5 km. The primary component of the monitoring program, the 4D surface seismic survey using a permanently deployed geophone array (Pevzner et al., 2017), successfully detected 5 kt of the injected CO_2 and tracked the CO_2 plume evolution and its post-injection stabilisation. Simultaneously with the surface seismic acquisition, the program included testing 3D VSP monitoring techniques using 3C borehole geophones and DAS (Correa et al., 2019, 2017; Tertyshnikov et al., 2018).

The shortcomings of the conventional 4D seismic are addressed by Otway Stage 3 Project which aims to demonstrate and validate the application of cost-effective technologies for subsurface monitoring and verification of a CO_2 storage site that also minimise environmental footprint. To this end, Stage 3 involves 15 kt of CO_2 injection (similar to Stage 2C but 600 m down-dip) but monitored primarily

from wells, with little infrastructure on or near the surface. The seismic monitoring in Stage 3 consists of two main components: continuous multi-offset VSP using five borehole DAS arrays and nine permanently installed Surface Orbital Vibrators (SOV) (Correa et al., 2021; Freifeld et al., 2021), and 4D VSP using mobile vibroseis source and the same DAS arrays. Details of operations and initial results of Stage 3 have been reported by Pevzner et al. (2022, 2021), Isaenkov et al. (2021) and Yavuz et al. (2021).

Data acquisition

The 4D VSP monitoring program of the Otway Stage 3 Project includes acquisition of a baseline M6 survey and two monitor surveys M7 and M8 after injection of 4 kt and 12 kt of CO_2, respectively. The survey parameters are shown in Table 1. The receiver arrays consist of engineered fibre-optic cables cemented behind the casings of five wells drilled to the depths from 1580 m to 1690 m. The configuration of the receiver arrays is the same as for the continuous DAS/SOV monitoring and was reported by Isaenkov et al. (2021). Note that the nearly vertical CRC-3 well instrumented with a DAS array is also an injector in Stage 3.

The parameters of the seismic source effort are shown in Table 2. The lateral distribution of seismic shot points and the projections of the receiver arrays to the surface are shown in Figure 1. The acquisition of a baseline M6 survey was disrupted by the onset of the COVID-19 pandemic in Australia in March 2020 (Pevzner et al., 2021). The original plan of acquiring more than 4,500 shots was revised because of delays in acquisition related to COVID-19 restrictions and rapidly deteriorating weather and ground conditions typical for this time of the year. The total M6 survey source effort included 3,395 shots with a lower source density compared to the original plan, but similar areal coverage. A previous analysis showed that this reduction in source density should have only a mild impact on the image quality (Popik et al., 2019).

The Stage 3 injection started in December 2020. The first monitor (M7) survey was acquired in January 2021 after injection of 4,382 t of CO_2. As flow simulations and preliminary results of the

continuous monitoring showed the CO_2 plume to still be relatively small, far-offset shot points on the eastern and western flanks were excluded to reduce the duration of the survey. On the other hand, the source coverage in the middle of the survey area was restored to the original M6 plan. The second monitor (M8) survey was acquired in March 2021 after injection of 12,465 t of CO_2 and included all the shot points from M6 and M7 surveys.

Table 1. Survey parameters.

Survey	M6	M7	M8
Date	March-April 2020	January 2021	March 2021
Wells	CRC-3, CRC-4, CRC-5, CRC-6, CRC-7		
Type of fibre	Constellation		
DAS interrogator	iDAS v3		
Measurand	Strain rate		
Gauge and pulse length	10 m gauge length, 4 m pulse length		
Channel spacing	1 m		
Temporal sampling	1 kHz (downsampled from 16 kHz laser pulse repetition frequency during acquisition)		
Source line spacing	~100 m		
Shot interval	15 m		
Number of shot points	3395	3085	4185
Survey area (km^2)	7.3	5.4	7.3

Table 2. Source parameters.

Seismic source	INOVA UniVib 26,000 lbs

Sweep type	Linear, 6-150 Hz
Sweep duration	24 s, 0.5 s cosine taper
Sweeps per shot point	1, 70% peak force

131

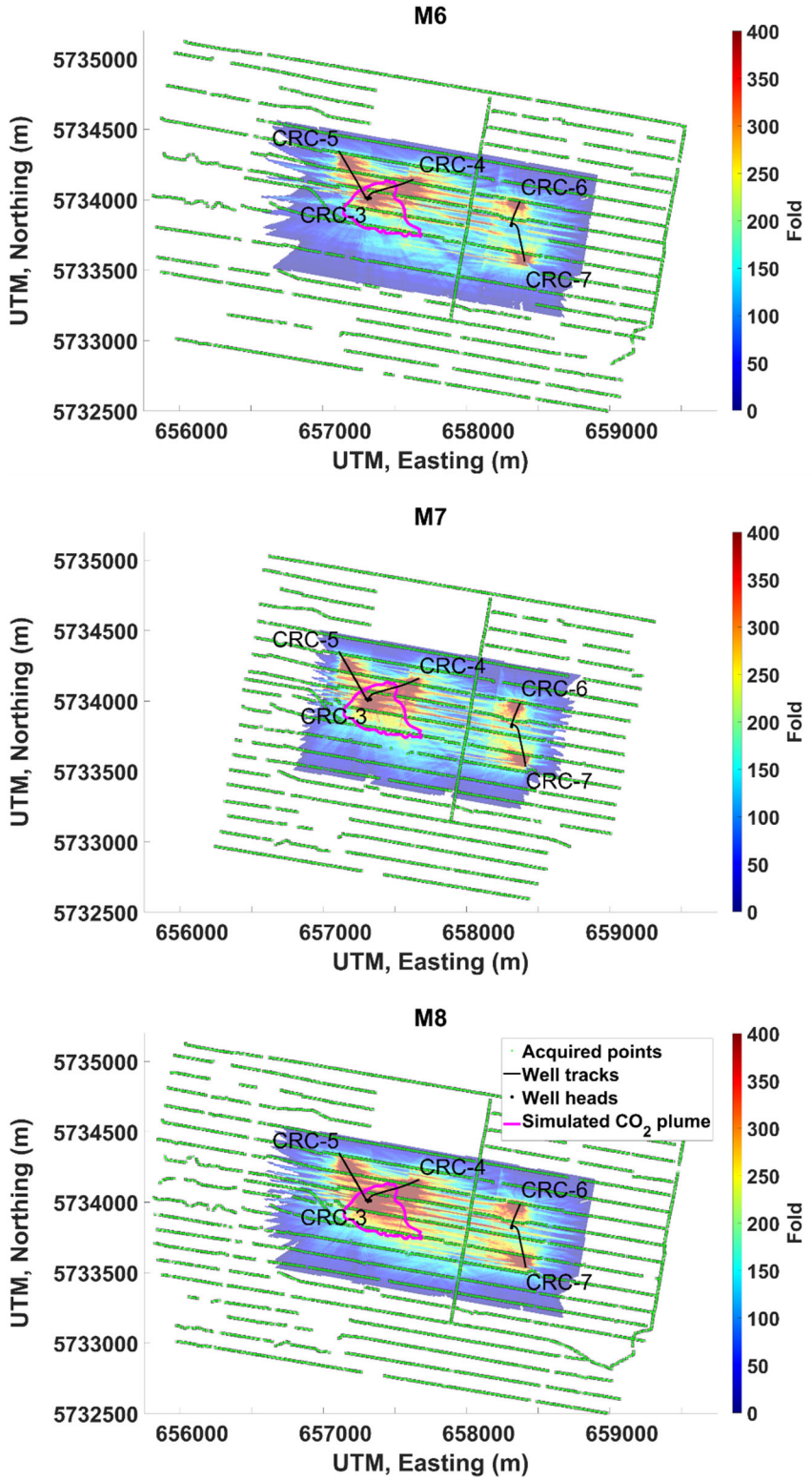

Figure 1. Lateral distribution of seismic shot points (green dots). Black lines show the projection of the wells' tracks to the surface. Color-coded map shows seismic fold computed for receiver spacing of 5 m and 7.5 × 7.5 m bin size, combined for all wells. The pink contour shows the projection of the edge of the simulated plume at the end of the injection. Modified after Pevzner et al. (2021).

Processing of the time-lapse DAS VSP data

To obtain a time-lapse image of the subsurface after injecting 4 kt and 12 kt of CO_2, we used the M6 dataset as a baseline for the M7 and M8 surveys. Additionally, we subtracted the M7 image from M8 to track the changes in the reservoir in the period between acquisition of these two monitors. Each dataset contains seismic records from five monitoring wells, which were processed separately.

To perform a parallel processing of the datasets, we used the RadExPro (DECO Geophysical) software package and in-house Matlab codes. The processing workflow (Figure 2) for each vintage was based on the fast-track processing of the Otway multi-well 3D VSP data reported by Yurikov et al. (2021).

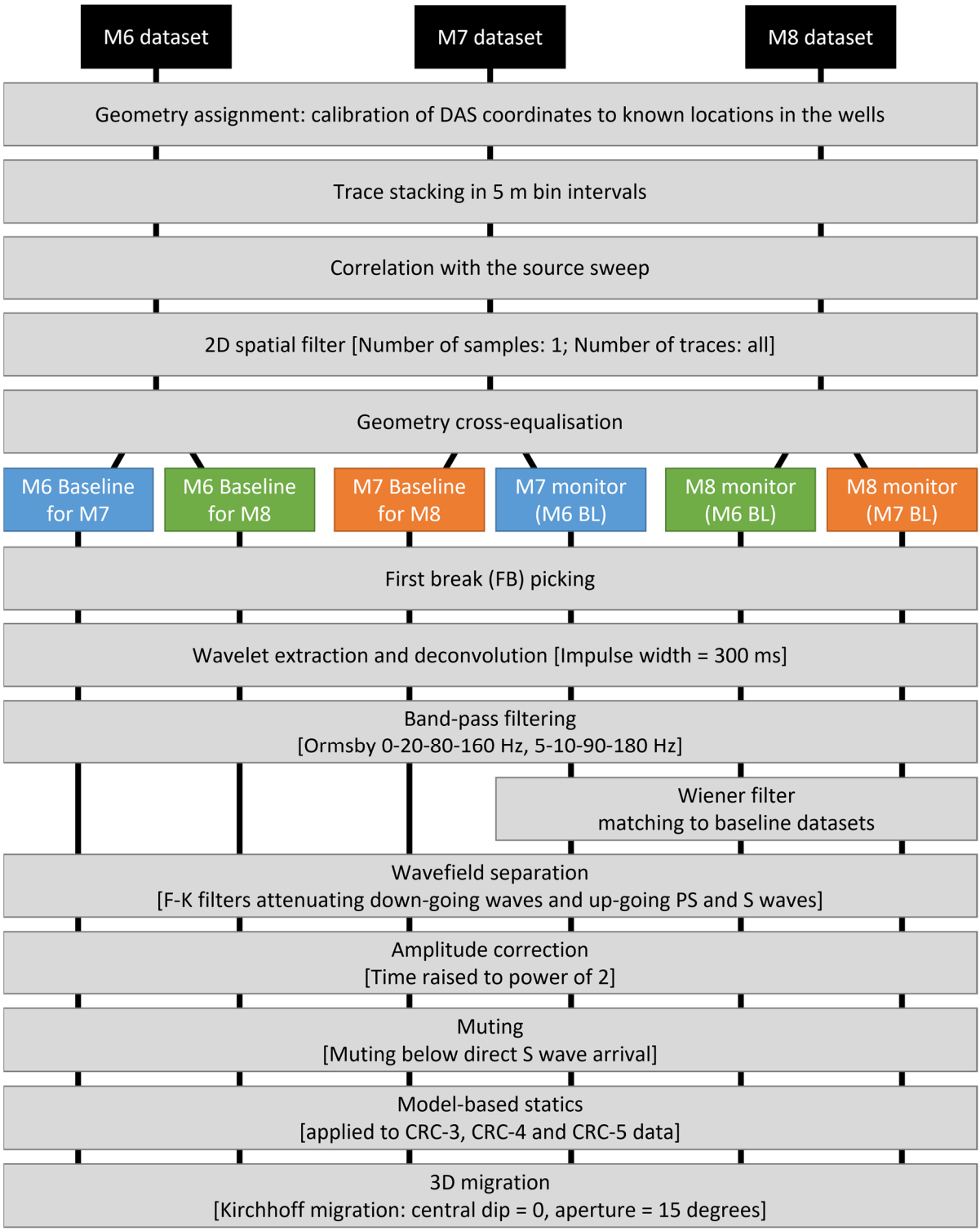

Figure 2: Processing flowchart: procedures are shown in grey boxes, initial datasets are shown in black boxes, datasets with cross-equalised geometries forming three baseline-monitor pairs are shown in blue, green and orange boxes.

The data was recorded in the iDAS v3 native TDMS format and then converted to SEG-Y. The coordinates of the source positions were obtained from the Differential Global Positioning System (DGPS) surveying. The geometry on the optic sensors was calibrated by pinpointing specific positions on the cable to known locations in the wells. Noisy traces were deleted from the datasets. In case of the repeated shots the one with the higher S/N ratio was taken into the further processing sequence. Raw traces were stacked within 5 m depth intervals and correlated with the source sweep. Then, the 2D spatial filter was applied to each shot gather targeting to attenuate the stripe noise present in the raw data.

Then we cross-equalised geometries of the surveys producing three baseline-monitor pairs of datasets for further analysis (M7-M6, M8-M6 and M8-M7). Because of the differences in source coverage (Figure 1), these survey combinations contain 2,586 shots for the M7-M6 pair, 3,358 shots for the M8-M6 pair and 3,085 shots for the M8-M7 pair.

The next step of the processing was a deterministic deconvolution. The source wavelets for the deconvolution were extracted from direct-wave arrivals for each shot gather by flattening first breaks and stacking traces recorded at depths over 1,200 m. Then, the wavelets extracted from different wells were averaged for each shot point and normalised relative to their root mean square (RMS) value. A wavelet was excluded from the averaging if the offset between a corresponding shot point and a well exceeded 1,500 m. The deterministic deconvolution corrected the phase of the data and widened the amplitude spectrum. The deconvolution also partially compensated for the effect of variations in the near-surface conditions on the source signature, which may be significant (Isaenkov et al., 2021). After deconvolution, we apply bandpass filters to attenuate the high-frequency noise.

To increase the repeatability of the data and further reduce the effect of changing near-surface conditions on the source signature, the monitor datasets are subjected to a matching Wiener filtering

174 $$D(t,l) * F(t), \quad (1)$$

175 where $F(t)$ is the filter, $D(t,l)$ is the data after deconvolution stage of the processing, t is the time,
176 and l is the measured depth along the well. To minimise the difference between the wavelets
177 extracted from the baseline $w_b(t)$ and the monitor data $w_m(t)$, the filter was designed for each shot
178 separately

179 $$\|w_b(t) - w_m(t) * F(t)\|_{L_2} \to 0. \quad (2)$$

180 The wavelets were extracted using the direct P-waves recorded below 800 m in every well
181 separately. We selected the part of each trace in the data in a window from -50 ms to 350 ms
182 relative to the picked first breaks. The traces with no first breaks picked due to low S/N ratio for the
183 direct P-wave were excluded from the analysis. We aligned the traces in time relative to the first
184 breaks and took their trimmed mean using 30% cut-off. For the CRC-3 well, only traces recorded
185 above the injection interval were used as the traces recorded below might be affected by time-lapse
186 changes related to the CO_2 injection. Then we derived a 150 ms long Wiener filter for each shot
187 using equation (2) and applied it to the monitor datasets (1).

188 Figure 3 shows an example of the wavelets extracted from the M7 and M8 datasets for one shot
189 location. There is a significant difference between the wavelets, which is minimised by applying the
190 matching filter. Applying the same filter to the whole monitor shot record significantly improves
191 repeatability (Figure 4).

192 The next processing step was the wavefield separation using F-K filters. The first pass F-K filter was
193 applied to shot gathers for attenuating all down-going waves. The second pass of F-K was applied to
194 shot gathers with flattened PP waves to remove up-going PS and S waves. The amplitude decay due
195 to the divergence of the wavefront was compensated with a time-squared function. Due to the
196 difficulty of removing the up-going S waves, we muted the data after the direct arrival of the S wave.

Prior to migration, we introduced the model-based static correction to the data. For every shot, we calculated the travel-time curves for the direct P wave using the same velocity model as used in the migration algorithm. Then we computed the misfits between the picked first breaks and the travel-time curves for each shot separately in the depth interval below 1,400 m. We took the 33% trimmed mean of these misfits and applied the result as a static shift to both baseline and monitor data.

The imaging was done using an in-house Matlab implementation of a Kirchhoff migration algorithm modified to correct for the directional dependency of DAS sensors (Bona et al., 2017; Kuvshinov, 2016). The correction was computed using the actual deviation of wells but assuming straight ray paths. The migration parameters included the central dip of 0° and the aperture of 15°. The data from each of the five wells were migrated independently on the common grid with 7.5m × 7.5m × 1m bin size. For migration of all datasets, we used a 1D isotropic velocity function derived from the zero-offset VSP in the CRC-3 well. The use of a 1D model is justified by relatively flat geology and modest lateral variation of the seismic velocities over the area (Dance, 2013).

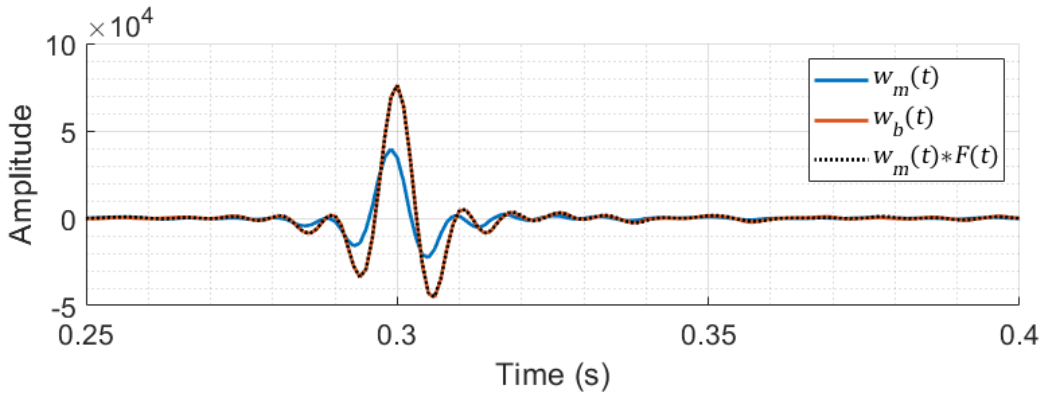

Figure 3: Example of the wavelets extracted from the M7 (w_b) and M8 (w_m) shot records from the same location. The result of applying a Wiener filter to the M8 wavelet shown by the black dotted line matches the M7 wavelet.

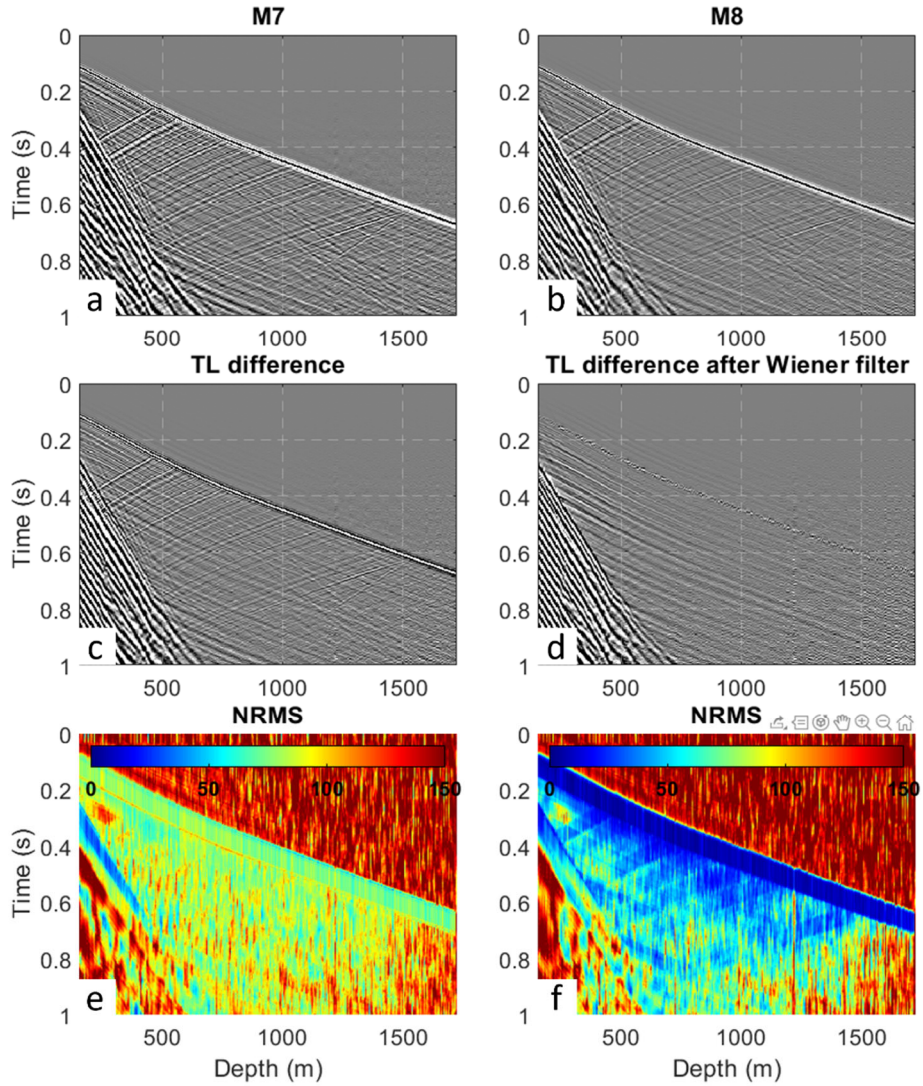

Figure 4: Example of the M7 (a) and M8 (b) shot records from the same location and their time-lapse (TL) difference before (c) and after (d) applying the Wiener filter. Time and depth variable gains were applied for visualisation purposes. The 60 ms window NRMS of the data before (e) and after (f) applying the Wiener filter is shown under corresponding difference images.

Results

Figure 5 shows a set of cross-sections of the seismic 3D volumes obtained using the M6 dataset. The sections are color-coded to differentiate between different volumes. The position of seismic reflectors is relatively consistent across the volumes. The quality of the images naturally degrades away from the corresponding well due to the VSP geometry, which makes it challenging to match

224 the volumes between the eastern (CRC-6 and CRC-7) and western (CRC-3, CRC-4 and CRC-5) groups
225 of wells. The discrepancies in the amplitudes of reflectors in different seismic volumes are related to
226 differences in illumination and effects of directivity of the fibre.

227 Figure 6 shows cross-sections of the migrated 3D time-lapse difference volumes for all three
228 baseline-monitor pairs M7-M6, M8-M6 and M8-M7. The data recorded in different wells were
229 processed separately from each other, hence Figure 6 displays images for all five monitoring wells.
230 The CO_2 plume was detected by time-lapse changes of reflection amplitudes in the injection interval.
231 Whereas the amplitude anomaly created by the injected gas is strong in the CRC-3 and CRC-4 data, it
232 is relatively weak in the CRC-5 data. The weakening of the time-lapse signal on the CRC-5 data has
233 two possible explanations. First, the positioning of the well relative to the plume is such that the
234 directional sensitivity of the fibre optic array has the most prominent effect on the CRC-5 time-lapse
235 data. Second, CRC-5 is also the only well where the interrogator was replaced between M6 and
236 M7/M8 surveys, which resulted in deteriorated repeatability of the data.

237 For each vintage, the plume was mapped using RMS amplitude attributes computed at the target
238 horizon from five seismic 4D volumes obtained from each of the monitoring wells (Figure 7). The
239 time-lapse signal is broadly consistent between different seismic volumes. However, due to
240 differences in well geometry, the directivity of fibre optic sensors and different illumination patterns,
241 the time-lapse signatures are not identical, but rather complement each other providing a broader
242 understanding of the plume's spatial extents.

243 Time-lapse difference volumes obtained using data recorded in CRC-6 and CRC-7 from M8-M7 pair
244 show a weak but clear time-lapse anomaly inside the Stage 2C CO_2 plume (Figure 6, Figure 7). The
245 location of the Stage 2C plume is known from 4D surface seismic data (Pevzner et al., 2017). First,
246 this result suggests that the Stage 3 plume has expanded eastward, connected with the Stage 2C
247 plume, and remobilised it. Second, we observe the time-lapse difference inside the Stage 2C plume.
248 Understanding of whether these changes are caused by thickening of the plume or increasing CO_2

saturation requires further quantitative investigation. It is important to mention that this time-lapse anomaly is weak and only marginally above the noise level (Figure 7). It was not detected in the M8-M6 pair because of the reduced source coverage in M6, which resulted in insufficient fold in the target area to the south-east of the injector. Increasing the source density by using M8-M7 datasets revealed a stronger time-lapse anomaly in between the two drill pads (CRC-3,4,5 and CRC-6,7) (Figure 6, Figure 7). This result confirms that 4D DAS VSP is a sensitive tool for reservoir monitoring and it has a potential to enable detection of gas-to-gas injection.

Combining all available information from all the wells and datasets gives the 3D distribution of the injected CO_2 in the subsurface (Figure 8). The results show that the plume primarily moves to the east in the up-dip direction of the subsurface structure until it reaches the Stage 2C plume and remobilises it. The Stage 3 plume is likely trapped by a regional fault at the south.

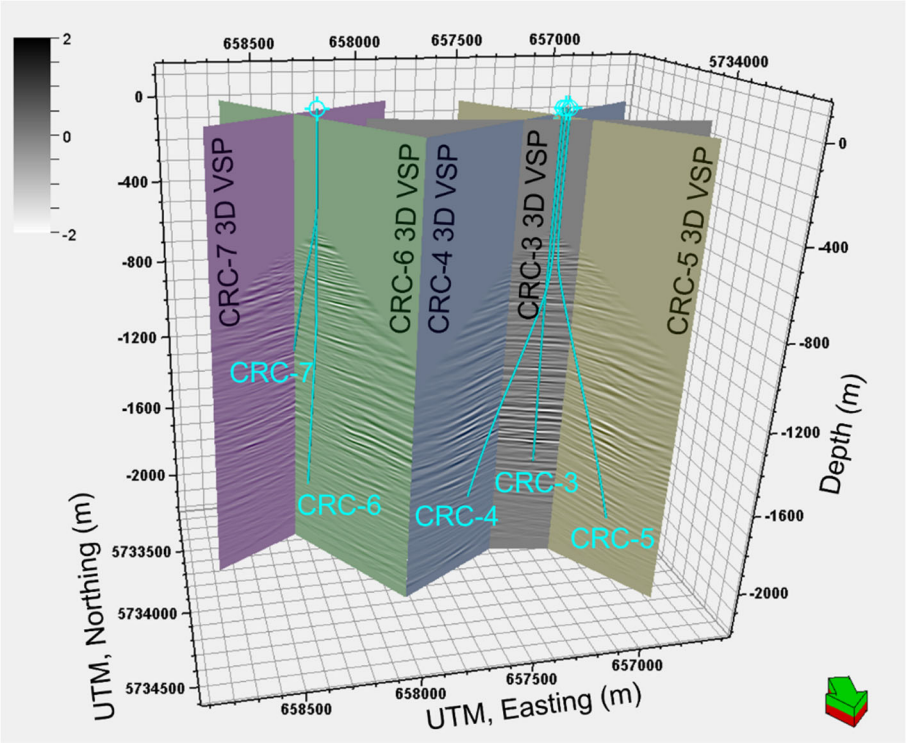

Figure 5: Cross-sections of the migrated M6 3D DAS VSP volumes from five wells: CRC-3 (grey), CRC-4 (blue), CRC-5 (yellow), CRC-6 (green), CRC-7 (purple).

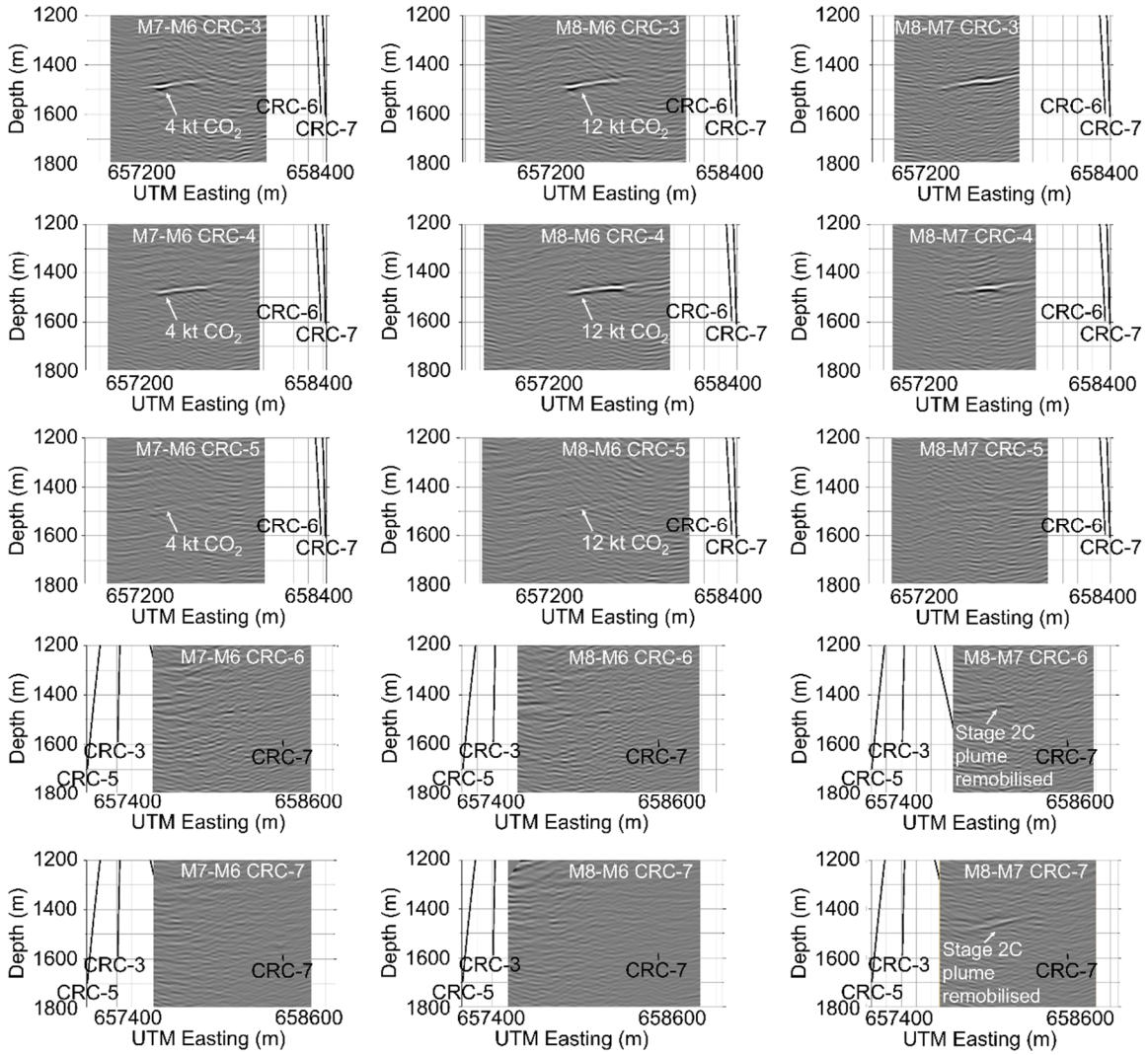

Figure 6: Time-lapse differences seismograms obtained using M6, M7 and M8 datasets: vertical slice through the injector well in the west-east direction (A-A' in Figure 7).

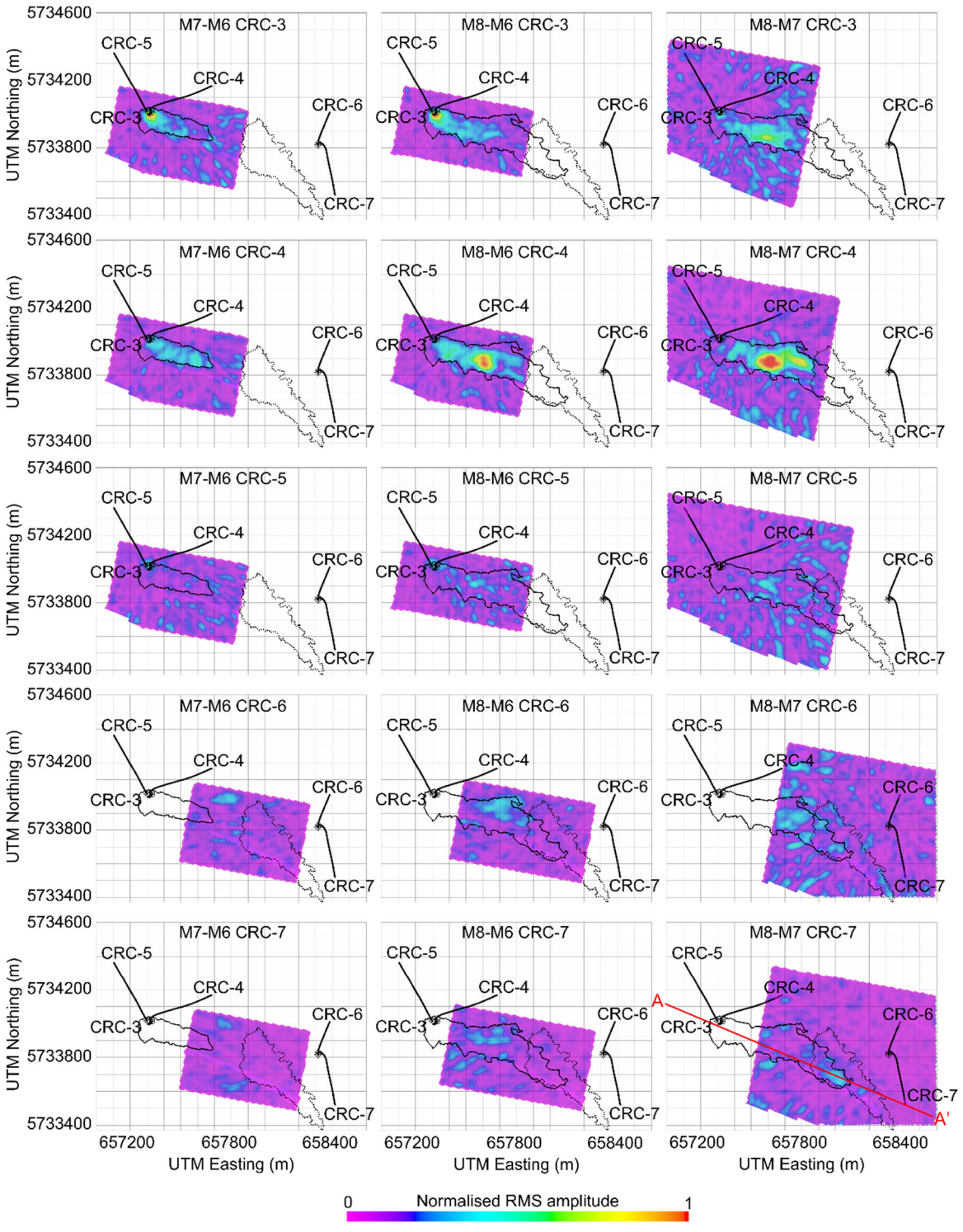

267

268 *Figure 7: RMS amplitude attributes of the time-lapse differences computed at the target horizon for CRC-3-7 wells from 4D*

269 *VSP. The black solid contours outline the extents of the interpreted Stage 3 CO_2 plume. The black dashed contour shows the*

270 *location of the Stage 2C plume.*

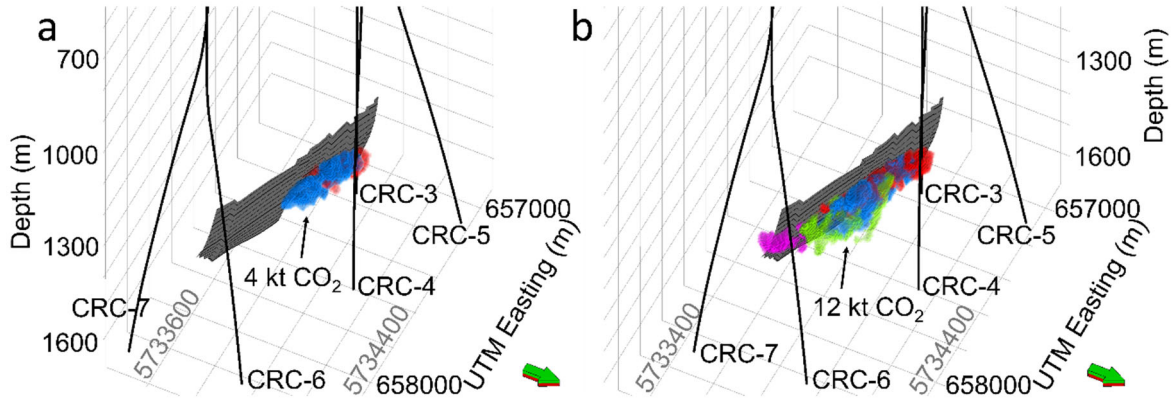

Figure 8: 3D representation of the interpreted Stage 3 plume after injection of 4 kt CO_2 (a) and 12 kt CO_2 (b). The color-code of the geobodies corresponds to the well data: red for CRC-3, blue for CRC-4, green for CRC-6, and purple for CRC-7. The black plane on the image is the part of the regional Splay fault, which possibly traps the plume.

Discussion

Comparison of 4D DAS VSP and continuous multi-offset DAS VSP

The results of the 4D DAS VSP monitoring can be cross-validated with the results of the continuous seismic monitoring using offset DAS/SOV VSP. Figure 9 shows a juxtaposition of the difference seismograms obtained using the two methods. As expected, 4D VSP provides a higher spatial resolution, while continuous DAS/SOV monitoring provides a higher temporal resolution as the vintages are produced every two days (Pevzner et al., 2021). Figure 10 shows how the continuous offset VSP monitoring captures the extents of the CO_2 plume in comparison with the 4D VSP. The normalised RMS amplitude of the time-lapse signal detected on the DAS/SOV transects are color-coded. The time-lapse signature of the CO_2 plume is broadly consistent between 4D VSP monitoring and the continuous offset VSP monitoring using DAS/SOV arrays. As reported by Pevzner et al. (2021), the plume image obtained from offset VSP geometry looks slightly larger due to an attempt to image a small 3D object using only (pseudo) 2D geometry, so that reflection points located within the plume but outside of the imaging plane still contribute to the image. Both methods of monitoring capture time-lapse changes withing the Stage 2C plume confirming its remobilisation,

290 which, according to the data of continuous multi-offset VSP monitoring, occurred in February 2021,
291 before the M8 acquisition. The offset DAS/SOV method of monitoring provides up to fivefold
292 improvement of S/N ratio compared to 4D VSP (Pevzner et al., 2021), hence it can detect smaller
293 changes like those in the northern part of the Stage 2C plume, which were not captured by 4D VSP.

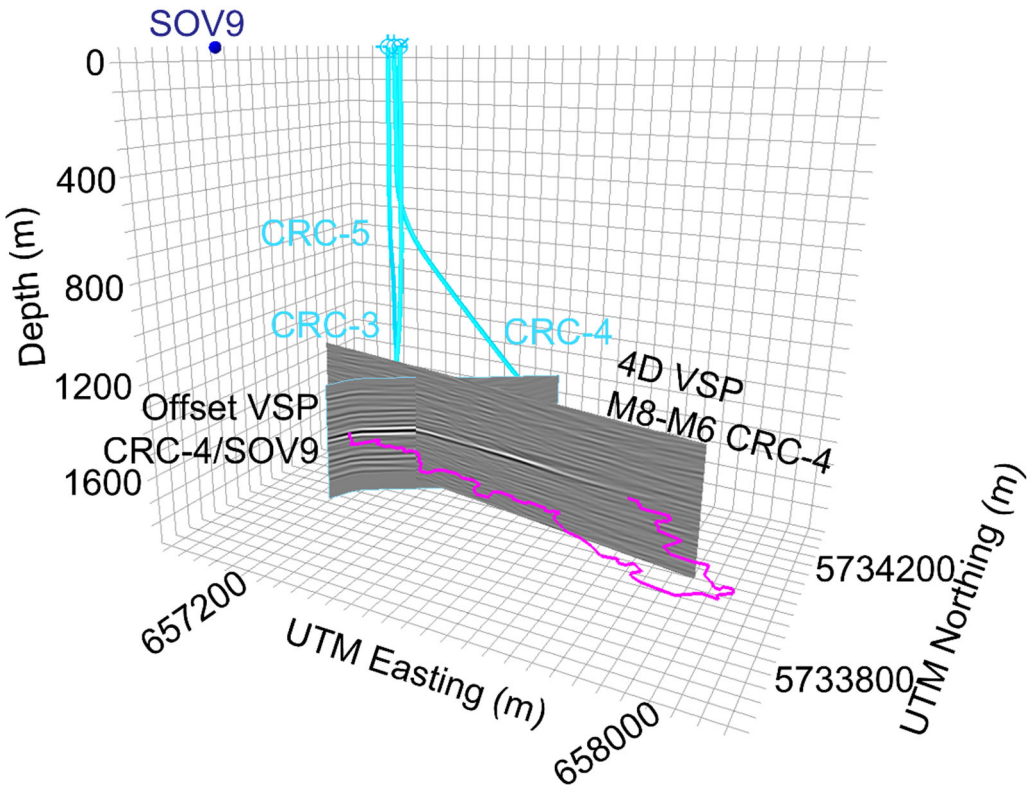

294

295 *Figure 9: Comparison of a migrated difference section of 4D VSP (CRC-4) for M8 dataset juxtaposed with the corresponding*
296 *offset VSP (CRC4/SOV9) section acquired one day before the M8 survey. Pink contour corresponds to the plume extend*
297 *interpreted from the 4D VSP data.*

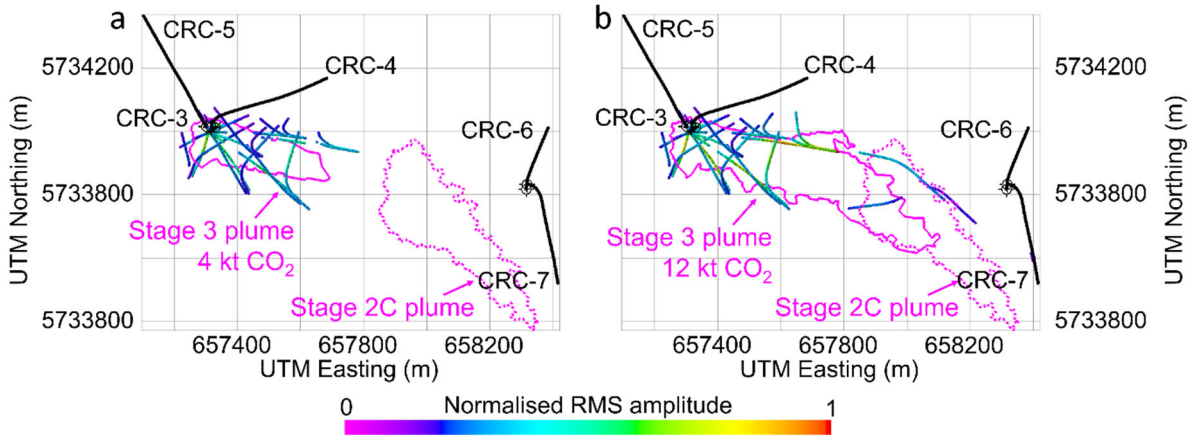

298

299 *Figure 10: Comparison of the evolution of the CO_2 plume captured by the 4D VSP and continuous offset VSP monitoring. The*
300 *colour code shows the normalised RMS amplitude of the time-lapse signal at the DAS/SOV transects. The dashed pink*
301 *contour shows the spatial extents of the Stage 2C plume detected by the 4D surface seismic. The solid pink contours show*
302 *the extents of the Stage 3 plume as detected by the 4D VSP.*

303 *Challenges of using 4D DAS VSP as a seismic monitoring tool*

304 An important parameter for any time-lapse seismic monitoring is repeatability of the data. Isaenkov
305 et al. (2021) analysed repeatability of continuous DAS/SOV monitoring and showed that the source
306 signature and repeatability are sensitive to weather changes. It is logical to assume that the same is
307 also true for vibroseis data. Changing precipitation and depth of the water table affect near-surface
308 conditions and hence coupling of the vibroseis with the ground and a character of the primary and
309 secondary wavefield. In case of VSP, seismic receivers are positioned in the subsurface and record
310 the direct as well as reflected waves. As demonstrated in Figure 4, the source signature extracted
311 from the direct wave arrival can be used to compensate for the near-surface variations and boost
312 the repeatability of the seismic data This step appears to be crucial for detection and tracking small
313 time-lapse changes in the subsurface.

314 Another challenge for the multi-well 4D VSP monitoring is the variation of the plume's shape from
315 well to well. As reported by Pevzner et al. (2021), the Stage 3 plume is a spatially small object, with
316 lateral dimensions of only a few hundred meters, so changes in illumination and imperfection of the
317 1D velocity model affect the final image. The Otway area is also known to have significant vertical

and azimuthal seismic anisotropy (Popik et al., 2021), which is not yet accounted for in the imaging. The ability to focus the image of a small 4D object using multiple wells can be used as a tool to QC the velocity model and provide an estimate of the monitoring uncertainty.

Diminished time-lapse signal in the CRC-5 data (relative to CRC-3 and CRC-4 data) (Figure 5) highlights another possible limitation in the 4D DAS VSP system – whereby once a single baseline is established, a change of the interrogator (for any reason) for subsequent monitors may introduce significant time-lapse errors. At the current stage of DAS technology, this appears to be an inherent issue in the interrogator designs, which cannot easily be corrected for by a simple calibration. Further research is required to understand if this technology can be applied in a "plug and play" manner or further development by the manufacturer of these units would allow this functionality.

Conclusions

The seismic monitoring program of the CO_2 injection in the Stage 3 of the Otway project includes 4D VSP using mobile vibroseis sources and five downhole DAS receiver arrays. Its primary purpose was to benchmark the results of the continuous multi-offset VSP monitoring with permanent SOV sources. Three vintages of 4D VSP seismic data were acquired before and during the injection, followed by fast-track data processing and analysis.

The initial analysis reveals that data repeatability suffers from changes in the near-surface conditions between acquisition campaigns. However, the effect of these changes can be compensated for by using direct-wave arrivals recorded in the borehole; this improves data repeatability significantly. Such compensation is an important processing step if small time-lapse changes are the target of monitoring.

The data recorded in different wells were processed independently using the same workflow. The obtained seismic volumes provide broadly consistent images of the CO_2 plume. However, these images are not identical because of differences in illumination of the target horizon and limitations

imposed by using a 1D velocity model in a complex anisotropic subsurface environment. The discrepancy in the plume images can potentially be used for QC and updating the velocity model and imaging techniques.

Images of the plume obtained using data from different wells complement each other providing a broader understanding of the location of the injected gas in the subsurface. For example, the western group of wells (CRC-3,4,5) provide detailed information at the beginning of injection when the plume is confined to the vicinity of CRC-3, whereas it cannot be detected from the eastern group of wells (CRC-6,7). With the propagation of the plume to the east, the data from the eastern wells captures the time-lapse changes, which are no longer detected by the western wells.

The 4D VSP data from CRC-6 and CRC-7 have also captured time-lapse changes that occurred inside the Stage 2C plume injected earlier into the same target reservoir ~600 m to the east from the Stage 3 injection. This time-lapse signal suggests that the Stage 3 plume has reached the Stage 2C plume and remobilised it. This conclusion is confirmed by the results of continuous monitoring using multi-offset VSP with SOV sources. Absence of any time-lapse changes in the Stage 2C plume before February 2021 confirms that the Stage 2C plume was stable before that date. This demonstrates that fibre-optic DAS receivers permanently installed in the subsurface have a potential for monitoring injection of gas into gas-saturated reservoirs.

Acknowledgments

The Otway Project received CO2CRC funding through its industry members and research partners, the Australian government under the CCS Flagships Program, the Victorian State government, and the Global CCS Institute. The authors wish to acknowledge financial assistance provided through Australian National Low Emissions Coal Research and Development. ANLEC R&D is supported by Low Emission Technology Australia (LETA) and the Australian Government through the Department of Industry, Science, Energy and Resources. Funding for LBNL was provided through the Carbon Storage Program, U.S. DOE, Assistant Secretary for Fossil Energy, Office of Clean Coal and Carbon

Management through the NETL, under contract No. DE-AC02- 05CH11231. The authors thank Michael Mondanos and Stoyan Nikolov (Silixa Inc.) for help with the fibre-optic equipment and Peter Dumesny (Upstream Production Solutions) for invaluable help with all aspects of field operations. The authors would like to thank Boris Gurevich for his highly valuable feedback and suggestions on this work.

References

Bacci, V.O., O'Brien, S., Frank, J., Anderson, M., 2017. Using a Walk-away DAS Time-lapse VSP for CO2 Plume Monitoring at the Quest CCS Project. Recorder 42, 18–21.

Bauer, R.A., Will, R., Greenberg, S.E., Whittaker, S.G., 2019. Illinois Basin–Decatur Project. Geophysics and Geosequestration 339–370. https://doi.org/10.1017/9781316480724.020

Bona, A., Dean, T., Correa, J., Pevzner, R., Tertyshnikov, K. v., van Zaanen, L., 2017. Amplitude and phase response of DAS receivers. 79th EAGE Conference and Exhibition 2017, 1–5. https://doi.org/10.3997/2214-4609.201701200

Bourne, S., Crouch, S., Smith, M., 2014. A risk-based framework for measurement, monitoring and verification of the Quest CCS Project, Alberta, Canada. International Journal of Greenhouse Gas Control, 26, 109-126. https://doi.org/10.1016/j.ijggc.2014.04.026

Chadwick, A., Williams, G., Delepine, N., Clochard, V., Labat, K., Sturton, S., Buddensiek, M.L., Dillen, M., Nickel, M., Lima, A.L., Arts, R., Neele, F., Rossi, G., 2010. Quantitative analysis of time-lapse seismic monitoring data at the Sleipner CO2 storage operation. Leading Edge (Tulsa, OK) 29, 170–177. https://doi.org/10.1190/1.3304820

Cook, P.J. (Ed.), 2014. Geologically storing carbon: learning from the Otway project experience. CSIRO Publishing.

Correa, J., Egorov, A., Tertyshnikov, K., Bona, A., Pevzner, R., Dean, T., Freifeld, B., Marshall, S., 2017. Analysis of signal to noise and directivity characteristics of das VSP at near and far offsets-A

CO2CRC Otway Project data example. Leading Edge 36, 994a1-994a7. https://doi.org/10.1190/TLE36120994A1.1

Correa, J., Isaenkov, R., Yavuz, S., Yurikov, A., Tertyshnikov, K., Wood, T., Freifeld, B.M., Pevzner, R., 2021. Distributed acoustic sensing/surface orbital vibrator: Rotary seismic sources with fiber-optic sensing facilitates autonomous permanent reservoir monitoring. Geophysics 86, P61–P68. https://doi.org/10.1190/GEO2020-0612.1

Correa, J., Pevzner, R., Bona, A., Tertyshnikov, K., Freifeld, B., Robertson, M., Daley, T., 2019. 3D vertical seismic profile acquired with distributed acoustic sensing on tubing installation: A case study from the CO2CRC Otway Project. Interpretation 7, SA11–SA19. https://doi.org/10.1190/INT-2018-0086.1

Couëslan, M.L., Ali, S., Campbell, A., Nutt, W.L., Leaney, W.S., Finley, R.J., Greenberg, S.E., 2013. Monitoring CO2 injection for carbon capture and storage using time-lapse 3D VSPs. Leading Edge 32, 1268–1276. https://doi.org/10.1190/TLE32101268.1

Daley, T.M., Freifeld, B.M., Ajo-Franklin, J., Dou, S., Pevzner, R., Shulakova, V., Kashikar, S., Miller, D.E., Goetz, J., Henninges, J., Lueth, S., 2013. Field testing of fiber-optic distributed acoustic sensing (DAS) for subsurface seismic monitoring. Leading Edge 32, 699–706. https://doi.org/10.1190/TLE32060699.1

Daley, T.M., Miller, D.E., Dodds, K., Cook, P., Freifeld, B.M., 2016. Field testing of modular borehole monitoring with simultaneous distributed acoustic sensing and geophone vertical seismic profiles at Citronelle, Alabama. Geophysical Prospecting 64, 1318–1334. https://doi.org/10.1111/1365-2478.12324

Dance, T., 2013. Assessment and geological characterisation of the CO2CRC Otway Project CO2 storage demonstration site: From prefeasibility to injection. Marine and Petroleum Geology 46, 251–269. https://doi.org/10.1016

Dean, M., Tucker, O., 2017. A risk-based framework for Measurement, Monitoring and Verification (MMV) of the Goldeneye storage complex for the Peterhead CCS project, UK. International Journal of Greenhouse Gas Control, 61, 1-15. https://doi.org/10.1016/j.ijggc.2017.03.014

Freifeld, B., Isaenkov, R., Tertyshnikov, K., Yavuz, S., Shashkin, P., Yurikov, A., Sidenko, E., Wood, T., Correa, J., Barraclough, P., Pevzner, R., 2021. Using surface orbital vibrators and DAS for realizing permanent reservoir monitoring — Lessons from the CO2CRC Otway Project. Global Meeting Abstracts 210–213. https://doi.org/10.1190/SEGJ2021-056.1

Hartog, A.H., 2017. An introduction to distributed optical fibre sensors. An Introduction to Distributed Optical Fibre Sensors 1–440. https://doi.org/10.1201/9781315119014

Hopkins, J., Mateeva, A., Harvey, S., Kiyashchenko, D., Duan, Y., 2021, Maturing DAS VSP as an Onshore CCUS monitoring technology at the Quest CCS Facility. GeoConvention 2021.

IEA, 2012. Energy Technology Perspectives.

IEA, 2021, Global Energy Review 2021, IEA, Paris https://www.iea.org/reports/global-energy-review-2021.

IPCC, 2021: Climate Change 2021: The Physical Science Basis. Contribution of Working Group I to the Sixth Assessment Report of the Intergovernmental Panel on Climate Change [Masson-Delmotte, V., P. Zhai, A. Pirani, S.L. Connors, C. Péan, S. Berger, N. Caud, Y. Chen, L. Goldfarb, M.I. Gomis, M. Huang, K. Leitzell, E. Lonnoy, J.B.R. Matthews, T.K. Maycock, T. Waterfield, O. Yelekçi, R. Yu, and B. Zhou (eds.)]. Cambridge University Press, Cambridge, United Kingdom and New York, NY, USA, In press, doi:10.1017/9781009157896.

Isaenkov, R., Pevzner, R., Glubokovskikh, S., Yavuz, S., Yurikov, A., Tertyshnikov, K., Gurevich, B., Correa, J., Wood, T., Freifeld, B., Mondanos, M., Nikolov, S., Barraclough, P., 2021. An automated system for continuous monitoring of CO2 geosequestration using multi-well offset VSP with permanent seismic sources and receivers: Stage 3 of the CO2CRC Otway Project.

International Journal of Greenhouse Gas Control 108, 103317. https://doi.org/10.1016/J.IJGGC.2021.103317

Jenkins, C., Chadwick, A., Hovorka, S.D., 2015. The state of the art in monitoring and verification—Ten years on. International Journal of Greenhouse Gas Control 40, 312–349. https://doi.org/10.1016/J.IJGGC.2015.05.009

Jervis, M., Bakulin, A., Smith, R., 2018. Making time-lapse seismic work in a complex desert environment for CO2 EOR monitoring — Design and acquisition. The Leading Edge 37, 598–606. https://doi.org/10.1190/TLE37080598.1

Kuvshinov, B.N., 2016. Interaction of helically wound fibre-optic cables with plane seismic waves. Geophysical Prospecting 64, 671–688. https://doi.org/10.1111/1365-2478.12303

Landrø, M., Veire, H.H., Duffaut, K., Najjar, N., 2003. Discrimination between pressure and fluid saturation changes from marine multicomponent time-lapse seismic data. Geophysics 68, 1592–1599. https://doi.org/10.1190/1.1444973

Li, M., Wang, H., Tao, G., 2015. Current and Future Applications of Distributed Acoustic Sensing as a New Reservoir Geophysics Tool. The Open Petroleum Engineering Journal 8, 272–281. https://doi.org/10.2174/1874834101508010272

Lumley, D.E., 2001. Time-lapse seismic reservoir monitoring. Geophysics 66, 50–53. https://doi.org/10.1190/1.1444921

Lüth, S., Bergmann, P., Huang, F., Ivandic, M., Ivanova, A., Juhlin, C., Kempka, T., 2017. 4D Seismic Monitoring of CO2 Storage During Injection and Post-closure at the Ketzin Pilot Site. Energy Procedia 114, 5761–5767. https://doi.org/10.1016/J.EGYPRO.2017.03.1714

Majer, E.L., Daley, T.M., Korneev, V., Cox, D., Peterson, J.E., Queen, J.H., 2006. Cost-effective imaging of CO2 injection with borehole seismic methods. Leading Edge (Tulsa, OK) 25, 1290–1302. https://doi.org/10.1190/1.2360622

Mateeva, A., Lopez, J., Chalenski, D., Tatanova, M., Zwartjes, P., Yang, Z., Bakku, S., Vos, K. de, Potters, H., 2017. 4D das VSP as a tool for frequent seismic monitoring in deep water. Leading Edge 36, 995–1000. https://doi.org/10.1190/TLE36120995.1

Mathieson, A., Midgely, J., Wright, I., Saoula, N., Ringrose, P., 2011. In Salah CO2 Storage JIP: CO2 sequestration monitoring and verification technologies applied at Krechba, Algeria. Energy Procedia 4, 3596–3603. https://doi.org/10.1016/J.EGYPRO.2011.02.289

Michael, K., Avijegon, A., Ricard, L., Myers, M., Tertyshnikov, K., Pevzner, R., Strand, J., Hortle, A., Stalker, L., Pervukhina, M., Harris, B., Feitz, A., Pejcic, B., Larcher, A., Rachakonda, P., Freifeld, B., Woitt, M., Langhi, L., Dance, T., Myers, J., Roberts, J., Saygin, E., White, C., Seyyedi, M., 2020. A controlled CO2 release experiment in a fault zone at the In-Situ Laboratory in Western Australia. International Journal of Greenhouse Gas Control 99, 103100. https://doi.org/10.1016/J.IJGGC.2020.103100

Oldenburg, C.M., 2018. Are we all in concordance with the meaning of the word conformance, and is our definition in conformity with standard definitions? Greenhouse Gases: Science and Technology 8, 210–214. https://doi.org/10.1002/GHG.1773

Pacala, S., Socolow, R., 2004. Stabilization wedges: Solving the climate problem for the next 50 years with current technologies. Science 305, 968–972. https://doi.org/10.1126/SCIENCE.1100103

Parker, T., Shatalin, S., Farhadiroushan, M., 2014. Distributed Acoustic Sensing - A new tool for seismic applications. First Break 32, 61–69. https://doi.org/10.3997/1365-2397.2013034

Pevzner, R., Glubokovskikh, S., Isaenkov, R., Shashkin, P., Tertyshnikov, K., Yavuz, S., Gurevich, B., Correa, J., Wood, T., Freifeld, B., 2022. Monitoring subsurface changes by tracking direct-wave amplitudes and traveltimes in continuous DAS VSP data. Geophysics 87, A1–A6. https://doi.org/10.1190/GEO2021-0404.1

Pevzner, R., Isaenkov, R., Yavuz, S., Yurikov, A., Tertyshnikov, K., Shashkin, P., Gurevich, B., Correa, J., Glubokovskikh, S., Wood, T., Freifeld, B., Barraclough, P., 2021. Seismic monitoring of a small CO2 injection using a multi-well DAS array: Operations and initial results of Stage 3 of the CO2CRC Otway project. International Journal of Greenhouse Gas Control 110, 103437. https://doi.org/10.1016/J.IJGGC.2021.103437

Pevzner, R., Urosevic, M., Popik, D., Shulakova, V., Tertyshnikov, K., Caspari, E., Correa, J., Dance, T., Kepic, A., Glubokovskikh, S., Ziramov, S., Gurevich, B., Singh, R., Raab, M., Watson, M., Daley, T., Robertson, M., Freifeld, B., 2017. 4D surface seismic tracks small supercritical CO2 injection into the subsurface: CO2CRC Otway Project. International Journal of Greenhouse Gas Control 63, 150–157. https://doi.org/10.1016/J.IJGGC.2017.05.008

Popik, S., Pevzner, R., Bona, A., Tertyshnikov, K., Glubokovskikh, S., Gurevich, B., 2021. Estimation of P-wave anisotropy parameters from 3D vertical seismic profile with distributed acoustic sensors and geophones for seismic imaging in the CO2CRC Otway Project. Geophysical Prospecting 69, 842–855. https://doi.org/10.1111/1365-2478.13080

Popik, S., Popik, D., Pevzner, R., 2019. Effect of density of seismic sources on the quality of the 4D seismic data. 81st EAGE Conference and Exhibition 2019 2019, 1–5. https://doi.org/10.3997/2214-4609.201901581

Roach, L.A.N., White, D.J., 2018. Evolution of a deep CO2 plume from time-lapse seismic imaging at the Aquistore storage site, Saskatchewan, Canada. International Journal of Greenhouse Gas Control 74, 79–86. https://doi.org/10.1016/J.IJGGC.2018.04.025

Schrag, D.P., 2007. Preparing to Capture Carbon. Science 315, 812–813. https://doi.org/10.1126/SCIENCE.1137632

Tertyshnikov, K., AlNasser, H., Pevzner, R., Urosevic, M., Greenwood, A., 2018. 3D VSP for monitoring of the injection of small quantities of CO2 – CO2CRC Otway case study. 80th EAGE Conference

and Exhibition 2018: Opportunities Presented by the Energy Transition 2018, 1–5. https://doi.org/10.3997/2214-4609.201801470

White, D., Harris, K., Roach, L., Robertson, M., 2019. 7 years of 4D seismic monitoring at the Aquistore CO2 Storage Site, Saskatchewan, Canada. SEG Technical Program Expanded Abstracts 4918–4922. https://doi.org/10.1190/SEGAM2019-3216776.1

Yavuz, S., Isaenkov, R., Pevzner, R., Gurevich, B., Tertyshnikov, K., Yurikov, A., Correa, J., Wood, T., Freifeld, B., 2021. Processing of multi-well offset vertical seismic profile data acquired with distributed acoustic sensors and surface orbital vibrators: Stage 3 of the CO2CRC Otway Project case study. Geophysical Prospecting 69, 1664–1677. https://doi.org/10.1111/1365-2478.13141

Yurikov, A., Tertyshnikov, K., Isaenkov, R., Sidenko, E., Glubokovskikh, S., Barraclough, P., Shashkin, P., Pevzner, R., 2021. Multi-well 3D DAS VSP imaging with engineered fibres: CO2CRC Otway Project case study. Geophysics 86. https://doi.org/10.1190/GEO2020-0670.1

Zwartjes, P., Mateeva, A., Chalenski, D., Duan, Y., Kiyashchenko, D., Lopez, J., 2018. Frequent, multi-well, stand-alone 3D DAS VSP for low-cost reservoir monitoring in deepwater. SEG Technical Program Expanded Abstracts 4948–4952. https://doi.org/10.1190/SEGAM2018-2997061.1